Polish J. Chem., **77**, 1529–1546 (2003)

Theoretical (DFT *in Vacuo*) Studies on the Structure of 2-(β-Aminoethyl)-pyridine – an Agonist of the Histamine H_1 Receptor. Comparison with Experiment (FT-IR in Apolar Solvent)*

by E.D. Raczyńska[1], M. Darowska[1] and T. Rudka[2]**

[1]*Department of Chemistry, Agricultural University, Nowoursynowska 159c, 02-776 Warsaw, Poland*
[2]*Interdisciplinary Department of Biotechnology, Agricultural University, Rakowiecka 26/30, 02-528 Warsaw, Poland*

(Received April 20th, 2003; revised manuscript July 3rd, 2003)

Preliminary quantum-chemical calculations (DFT) were performed for 2-(β-aminoethyl)-pyridine (AEP). In calculations, rotational isomerism around the single C–C and C–N bonds of the chain aminoethyl group in AEP was considered. Nine stable conformations (four *trans* and five *gauche*) with similar Gibbs energies were found. For all of them, vibrational frequencies were calculated at the DFT(B3LYP)/6-31G* level. Infrared (FT-IR) spectra were recorded in apolar solvent (CCl_4) for various concentrations of AEP, and compared with those found by computations. The comparison shows that in apolar CCl_4 solution AEP exists as a mixture of different conformers. Analysis of the experimental stretching NH and CH vibrations, and the bending in-plane NH vibrations suggests that all nine conformers of AEP can be present in CCl_4 solution.

Key words: 2-(β-aminoethyl)-pyridine, rotational isomerism, DFT in *vacuo*, infrared spectra in apolar solvent

2-(β-Aminoethyl)-pyridine (AEP) is an agonist of histamine receptors [1]. It displays similar physiological effects as histamine (HA), binding with high affinity and specificity to the histamine H_1 receptor [2]. From the chemical point of view, AEP is a bifunctional nitrogen ligand which possesses two basic sites, the N-aza in the aromatic ring and the N-amino in the aliphatic side chain. Histamine has the same basic sites, the ring N-aza and the chain N-amino, but it is a trifunctional compound. It contains additionally the acidic amino group (NH) in the ring. The NH together with the C=N forms the amidine moiety (–NH–CH=N–) which complicates the acid-base equilibria in HA, and extends possibilities of interactions of HA on various specific receptors. Currently, there are known four histamine receptors: H_1, H_2, H_3 and H_4 [3–8]. The pharmacology of these receptors differs among animal species. Generally, the H_1 receptor mediates contractions of smooth muscles. The H_2 receptor controls the secretion by various glands. The H_3 receptor mediates the neurotransmitter properties. The H_4 receptor has recently been discovered and it is not yet well characteri-

---

* Dedicated to Prof. M. Szafran on the occasion of his 70th birthday.
**Author for correspondence.

zed. HA and AEP, interacting with the H_1 receptor, display properties of aliphatic amines with an aromatic ring as substituent. Presence of the amidine moiety in HA is not necessary for the H_1 receptor. However, the basic N-amino site in the side chain is essential for interactions with the H_1 receptor, containing hydrophilic and negatively charged pocket.

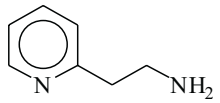

AEP

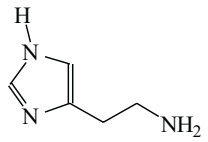

$HA\text{-}T_1$

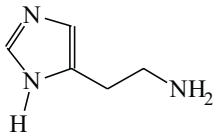

$HA\text{-}T_2$

To understand similarities and differences between AEP and HA in binding with the H_1 receptor, we have undertaken structural studies for both ligands. In our previous papers, rotational isomerism, intramolecular interactions and solvent effects have been discussed for HA [9–12]. It has been shown that conformational, tautomeric and basic preferences in gas phase and apolar solvents are not the same as in polar and H-bond donor or H-bond acceptor solvents. In the first case, HA prefers the *gauche* conformation, in which the ring N-aza takes the proton and the chain N-amino interacts with the protonated aza group [9–13]. In the other case, HA prefers the *trans* conformation with the chain N-amino more basic than the ring N-aza [11,12,14]. The *trans* conformation has also been suggested in the literature for the monocationic form [3–6] (which probably interacts with the hydrophilic and negatively charged pockets of the H_1 and H_2 receptors), and for the dicationic form [15,16] (which probably interacts with the histamine-binding proteins). Interacting with less hydrophilic pocket of the H_3 receptor, the monocationic form of HA takes probably the *gauche* conformation [4,7].

Lack of such information for AEP, encouraged us to start structural studies in a different environment. In this paper, quantum-chemical calculations were performed for isolated (*in vacuo*) AEP, and FT-IR spectra were recorded for solvated AEP (in apolar solvent). First, the semiempirical Austin Model 1 (AM1) [17] was applied to select all stable conformations possible for AEP in the gas phase. Next, the DFT (density functional theory) [18] with the B3LYP functional (the combination of the Becke three-parameter hybrid exchange functional with nonlocal correlation functional of Lee, Yang and Parr) [19] and the 6-31G* basis set [20] were used to optimize geometry of the selected stable conformations and to calculate vibrational IR spectra for the isolated (*in vacuo*) conformers. The DFT(B3LYP)/6-31G* has been found recently by Scott and Radom to be one of the most successful procedures for spectral analyses, and it has been recommended for interpretation of experimental IR spectra [21].

In parallel, FT-IR spectra were recorded in apolar solvent for different concentrations of free AEP. For measurements, CCl_4 was chosen as apolar, non-hydrogen bonding solvent, in which conformational preferences of AEP can be similar to those found by computations in the gas phase. Lack of the CH groups in CCl_4 allows us to

analyse the stretching CH vibrations of the chain dimethylene group, which are particularly sensitive to rotational isomerism. For analysis of both the theoretical and experimental IR spectra, the stretching NH and CH vibrations and the bending (in-plane) NH vibrations were selected, and their positions and intensities compared. This comparison, allowed us to indicate the conformations preferred by AEP in apolar solvent.

EXPERIMENTAL AND COMPUTATIONAL DETAILS

Materials. AEP (Aldrich) was distilled under reduced pressure and dried over molecular sieves (3 Å, 1 Å = 0.1 nm). CCl_4 (HPLC grade solvent of Aldrich) was dried over $LiAlH_4$ and distilled before use. Solutions were prepared in a dry glove-box.

Infrared measurements. FT-IR spectra were recorded using a Fourier transform spectrometer Perkin-Elmer 2000 with a 4 cm^{-1} resolution and 16 scans. All spectra were recorded at room temperature. The molar concentration of AEP varied from 0.001 to 0.1 mol dm^{-3}. Depending on concentration of AEP, different cells were applied: quartz cells of 1, 10 and 50 mm and KBr cells of 0.064, 0.625 and 2.66 mm. The ν(NH), ν(CH), and δ(NH) contours, selected for spectral analysis, were decomposed with help of the PEGRAMS program (working on the Perkin-Elmer 2000 system) using a mixture of Gaussian and Lorentzian functions.

Quantum-chemical calculations. To select all possible stable conformations of AEP, geometries of more than one hundred conformers of AEP were considered. Geometries of the stable AEP isomers were fully optimized without symmetry constraint, and vibrational frequencies calculated using the hybrid DFT functional B3LYP [18,19] and the 6-31G* basis set [20]. Fifty-five frequencies (calculated for each AEP isomer) were positive, indicating that the DFT optimized structures correspond to the energy minima. For DFT calculations, the GAUSSIAN 94 program [22] was applied. The DFT computed IR spectra for AEP isomers were produced from GAUSSIAN output files. To display the vibrational modes associated with calculated spectral lines, the MOLDEN program [23] installed on a two processor computer under the Linux system was used.

RESULTS AND DISCUSSION

Possible conformations for isolated (gas phase) AEP. 2-(β-Aminoethyl)-pyridine (AEP) is a very flexible bifunctional ligand. Similar to histamine (HA), it displays rotational isomerism around the single C–C and C–N bonds in the side chain (Figure 1). Depending on environment (gas phase or solution, metal or ammonium cation, hydroxide or carboxylate anion or other active site(s) in the H_1 receptor pocket) various conformations can be preferred by AEP.

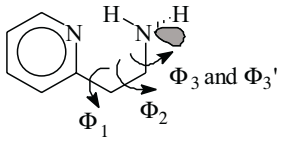

Figure 1. Starting positions for the Φ_1, Φ_2, Φ_3 and $\Phi_{3'}$ angles in AEP.

To select stable structures of AEP, more than one hundred conformations were considered. The representative conformations are given in Figure 2. Three angles (Φ_1, Φ_2 and Φ_3) were varied by 30° steps during the rotation around the chain C–C and C–N single bonds. The Φ_1 and Φ_2 angles correspond to the dihedral angles N(ring)–C(ring)–C(chain)–C(chain) and C(ring)–C(chain)–C(chain)–N(chain), re-

spectively. For clarity, two angles (Φ_3 and $\Phi_{3'}$) referring to the amino hydrogens were taken into account. They correspond to the dihedral angles C–C–N–H in the side chain. The starting positions for the Φ_1, Φ_2, Φ_3 and $\Phi_{3'}$ angles are given in Figure 1.

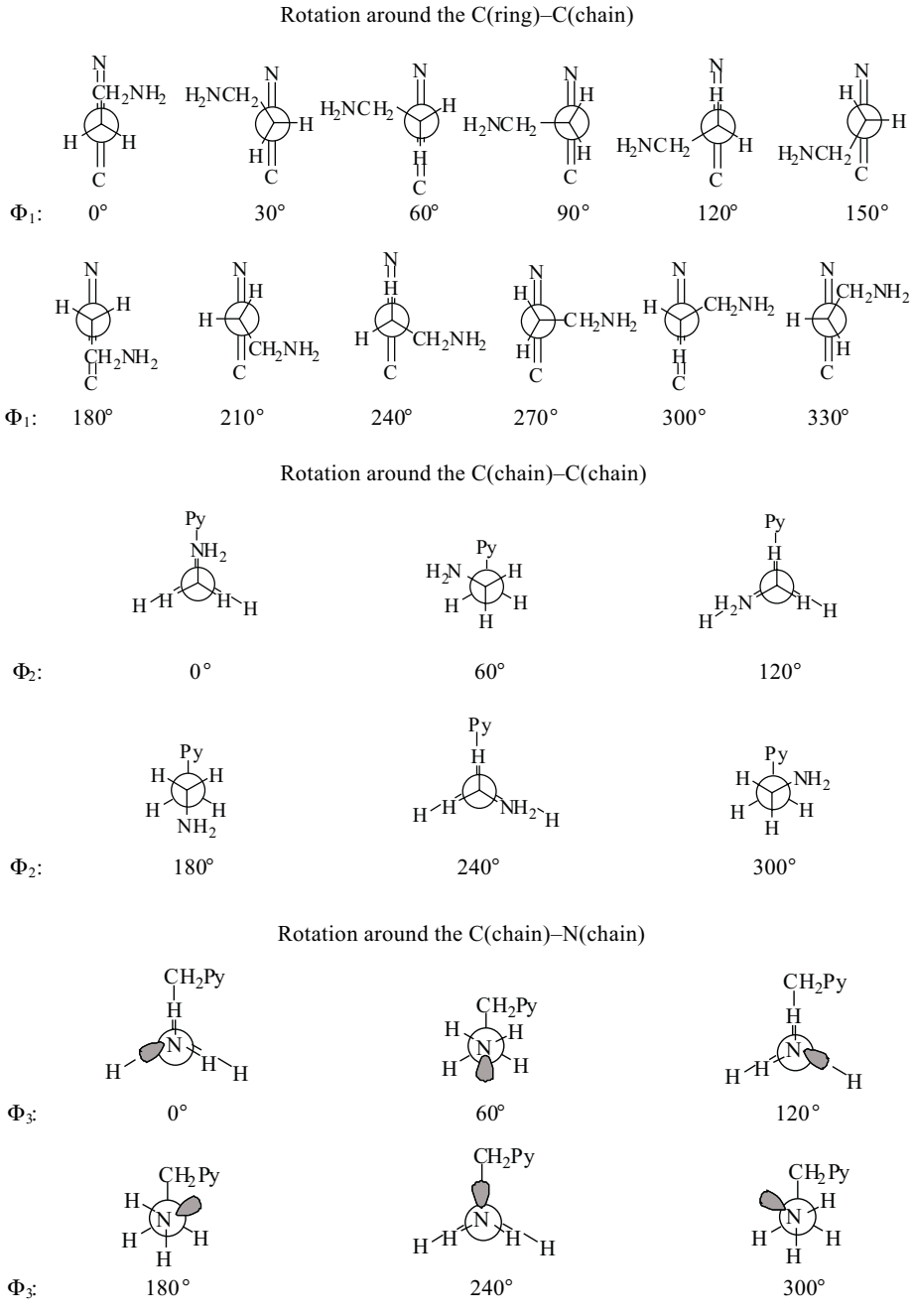

Figure 2. Representative conformations for the side chain aminoethyl group in AEP.

Preferred conformations for isolated AEP (DFT *in vacuo*). Due to a large number of AEP structures, the AM1 method [17] was applied to select all stable conformations of AEP. In this way, nine stable conformations of AEP were found, among which five are *gauche* and four are *trans*, similarly as in the case of the histamine tautomer HA-T_1 (in HA-T_1 the aminoethyl group is in 2-position *vis-á-vis* the aza group as in AEP) [10]). Next, the DFT(B3LYP) method [18,19] and the 6-31G* basis set [20] were applied to the stable structures of AEP selected by the AM1 method. The geometries were reoptimized without symmetry constraint and the stationary points on the potential energy surface were found. In this way, the same nine stable conformations were found for the free AEP (AEP1–AEP9 given in Figure 3). Five of them are *gauche* (AEP1–AEP5) and four are *trans* (AEP6–AEP9). The three *gauche* structures

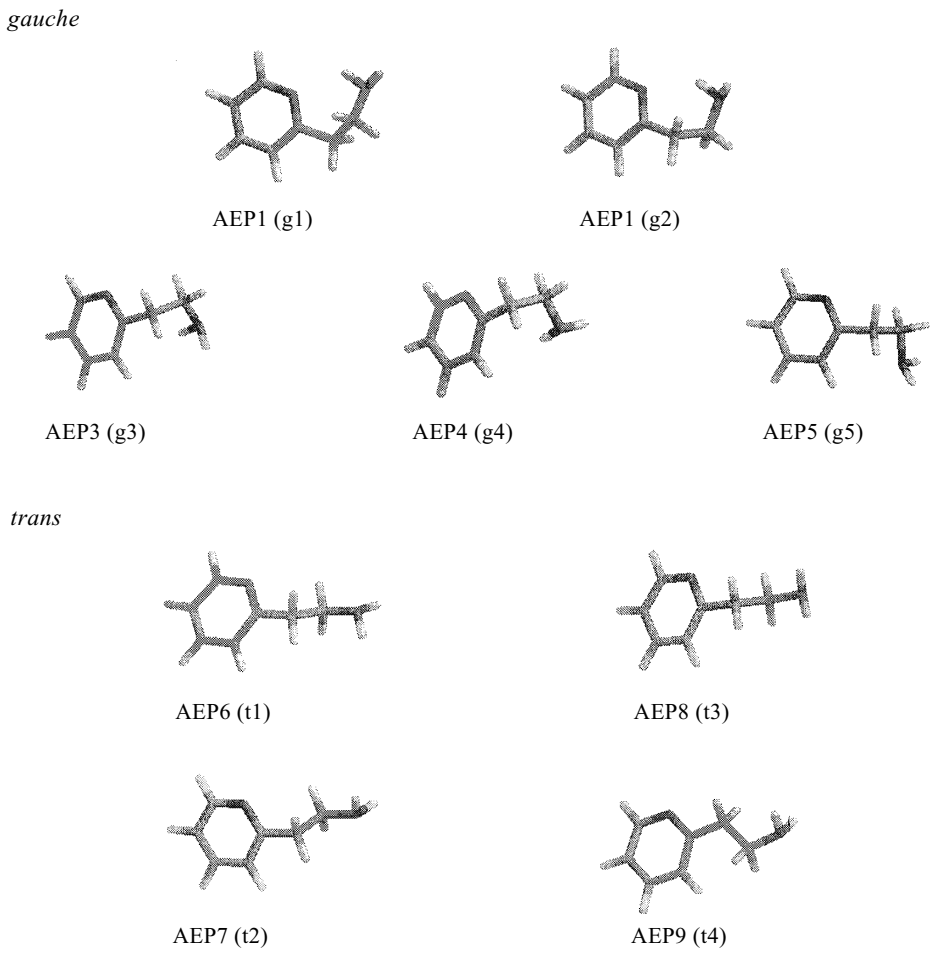

Figure 3. Stable structures found for 2-(β-aminoethyl)-pyridine (AEP) at the DFT(B3LYP)/6-31G* level.

AEP3–AEP5 differ mainly by conformation of the chain NH_2 group (Φ_3 and $\Phi_{3'}$ angles). The same is true for the three *trans* structures AEP6–AEP8.

Table 1 summarizes selected geometrical (angles Φ_1, Φ_2, Φ_3 and $\Phi_{3'}$) and physicochemical parameters (dipole moment μ, total energy E, relative Gibbs energy ΔG) obtained for the nine stable conformers of AEP at the DFT level. Comparison shows that the *gauche* structure AEP2 (g2) is the most stable one and corresponds to the global minimum. Among *trans* conformations, the *trans* structure AEP8 (t3 with slightly larger Gibbs energy than that of g2 by 0.4 kcal mol^{-1}) has the lowest energy.

Table 1. Selected geometrical (Φ_1, Φ_2, Φ_3 and $\Phi_{3'}$ angles given in Fig. 1) and physicochemical parameters (μ, E and ΔG) for the *gauche* and *trans* conformations of 2-(β-aminoethyl)-pyridine (AEP1–AEP9 given in Fig. 3) calculated at the DFT(B3LYP)/6-31G* level.

Isomer	Conformation	Φ_1[a]	Φ_2[a]	Φ_3[a]	$\Phi_{3'}$[a]	μ[b]	E[c]	ΔG[d]
AEP1	g1	35.1	–77.3	179.0	63.3	2.551	–382.260822	0.3
AEP2	g2	–64.7	69.3	64.1	–49.4	2.866	–382.261763	0.0
AEP3	g3	–75.3	–64.2	58.7	–57.8	2.797	–382.260359	0.5
AEP4	g4	–75.9	–66.3	68.5	–176.0	1.492	–382.260202	0.6
AEP5	g5	–88.5	–68.8	–75.2	168.6	1.833	–382.258753	0.6
AEP6	t1	–63.5	176.4	70.1	–174.1	2.672	–382.259134	1.0
AEP7	t2	–72.8	179.9	176.3	–68.2	1.248	–382.259641	0.8
AEP8	t3	–74.3	177.3	–59.0	57.2	2.506	–382.260414	0.4
AEP9	t4	180.0	180.0	57.7	–57.7	1.195	–382.2507631	1.4

[a]Angle in degree from the GAUSSIAN output file.
[b]Dipole moment in Debye (1 D = $3.33 \cdot 10^{-30}$ C m).
[c]Total energy in Hartree (1 Hartree = 627.5095 kcal mol^{-1}).
[d]Relative Gibbs energy in kcal mol^{-1} (1 cal = 4.184 J), ΔG = G(AEPi) – G(AEP2).

In the most stable AEP2 structure, both functional groups (the ring N-aza and the chain NH_2) interact by formation of intramolecular H-bonds. Distances between the ring N-aza and hydrogens of the chain NH_2 (both H in the *gauche* conformation to the CH_2Py) are equal to 2.34 and 3.43 Å. Similar interactions take place in the AEP1 *gauche* structure (g1 with the Gibbs energy slightly larger than that of g2 by 0.3 kcal mol^{-1}). Distances between the ring N-aza and hydrogens of the chain NH_2 (one H in the *gauche* and the other in the *trans* conformation to the CH_2Py) are equal to 2.28 and 3.77 Å.

Intramolecular interactions present in the other *gauche* structures AEP3 and AEP4 (g3 and g4 with larger Gibbs energies than that of g2 by 0.5 and 0.6 kcal mol^{-1}, respectively) are completely different than those in the AEP1 and AEP2 structures and also than those in the AEP5 structure (g5 with larger Gibbs energy than that of g2 by 0.6 kcal mol^{-1}). The chain NH_2 in AEP3 and AEP4 interacts with the π electrons of the pyridine ring, whereas the lone electron pair of the chain N-amino in AEP5 interacts with the pyridine ring.

For AEP3 (g3), the distances between one hydrogen of the chain NH_2 (in the *gauche* conformation to the CH_2Py) and the three ring atoms: N(1)-aza, C(2), C(3) are equal to 3.51, 2.82 and 3.05 Å, respectively. Distances for the other hydrogen of the chain NH_2 (also in the *gauche* conformation to the CH_2Py) and the ring atoms (1–3) are larger by *ca*. 1 Å. Similar behaviours are found for AEP4 (g4), for which distances between one hydrogen of the chain NH_2 (in the *gauche* conformation to the CH_2Py) and the ring atoms (1–3) are equal to 3.47, 2.76 and 2.98 Å, respectively. Distances for the other hydrogen of the NH_2 (in the *trans* conformation to the CH_2Py) are larger than 1 Å. Repulsion between the lone electron pair of the chain N-amino and the π electrons of the pyridine ring in AEP5 (g5) changes its geometry. Distances between the chain N-amino and the ring atoms (1–3) are slightly larger and equal to 4.05, 3.08 and 3.34 Å, respectively.

Although different interactions in the *gauche* structures (g1–g5) take place, their Gibbs energies are very close to each other ($\Delta G < 1$ kcal mol^{-1}). The Gibbs energies of the *trans* conformers (in which the intramolecular H-bonds are absent) only slightly differ from that of the most stable g2 ($\Delta G < 1.5$ kcal mol^{-1}). This suggests that all conformers of AEP may be present in the gas phase with preference of the g2 structure.

The g2 structure of AEP is also the most polar one ($\mu = 2.866$ D). Also the t3 structure of AEP, found as the most stable among the *trans* isomers, exhibits high polarity ($\mu = 2.506$ D). These facts should be taken into account in solution, in which conformation of AEP may depend on intermolecular interactions with solvent molecules (polar or apolar, H-bond donor or H-bond acceptor), and in which polarity of solute may play an important role.

In the case of free histamine tautomers (HA-T_1 and HA-T_2), ten stable conformations (seven *gauche* and three *trans*) have been found at the *ab initio* levels (RHF and MP2) [24]. The three *trans* conformations of HA-T_1 are similar to those (t1–t3) of AEP. Five (among seven) *gauche* conformations of HA-T_1 are similar to those (g1–g5) of AEP. The two other *gauche* conformations of HA-T_1 have not been found as stable for AEP. In rotational spectrum recorded in the gas phase (hot vapour), a mixture of four isomers of HA has been identified [24]. All of them have the *gauche* conformation and are stabilized by various intramolecular interactions between the chain NH_2 group and the imidazole ring (π-electrons, N-aza or NH group). In the mixture of these four conformers of HA, 15% has been assigned to the *gauche*-HA-T_1 structure, which is similar to the most stable g2 structure of AEP [24]. Larger percentage content has been found for the other tautomer, the *gauche*-HA-T_2 structure stabilized by the H-bond between the ring NH (H-bond donor) and the chain N-amino (H-bond acceptor). For this structure, the lowest energy was obtained at both the RHF and MP2 levels [24].

Aromatic character of the pyridine ring in DFT structures of AEP. As mentioned before, AEP is an agonist of the histamine H_1 receptor [1]. Investigations on HA, AEP and other histamine agonists and antagonists suggest that all biologically active derivatives, interacting with the H_1 receptor, display properties of aliphatic amines with an aromatic ring as substituent [2–4,16]. Although the chain NH_2 group

is essential for interactions with the active site of the H_1 receptor, the π electrons in the aromatic system play also an important role in binding with proteins and in activity of the drug [15,16]. For this reason, it is interesting to determine properties of the π electrons in AEP.

Aromatic character of the pyridine moiety can quantitatively be measured by the HOMA (Harmonic Oscillator Model of Aromaticity) index (close to 1 for benzene) [25–27]. In estimation of the HOMA index values in AEP isomers, equation (8) from ref. [25] and the new parameters for the C–C $\{\alpha(CC) = 257.7$ and $R(CC)_{opt} = 1.388\}$ and C–N bonds $\{\alpha(CN) = 93.52$ and $R(CN)_{opt} = 1.334\}$ were used. The estimations made for the DFT(B3LYP)/6-31G* structures of AEP (Table 2) show that independently on the conformation of the aminoethyl side chain the HOMA index is close to 1 for the pyridine ring (0.985 ± 0.001) similarly as for unsubstituted pyridine (0.998) [27]. For histamine species, the HOMA index is considerably lower (0.85 ± 0.05) [8], indicating smaller aromatic character of the imidazole ring.

Table 2. Bond lengths in the pyridine ring (in Å)[a] and HOMA indices calculated for the *gauche* and *trans* conformations of 2-(β-aminoethyl)-pyridine (AEP1–AEP9 given in Fig. 3) at the DFT(B3LYP)/6-31G* level.

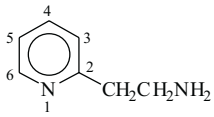

Isomer	C(2)–N(1)	C(6)–N(1)	C(2)–C(3)	C(3)–C(4)	C(4)–C(5)	C(5)–C(6)	HOMA
AEP1	1.345	1.338	1.403	1.392	1.395	1.393	0.984
AEP2	1.348	1.338	1.402	1.393	1.394	1.394	0.984
AEP3	1.346	1.336	1.402	1.395	1.393	1.396	0.985
AEP4	1.346	1.337	1.402	1.394	1.394	1.396	0.983
AEP5	1.344	1.338	1.401	1.392	1.395	1.394	0.987
AEP6	1.346	1.336	1.401	1.394	1.393	1.396	0.985
AEP7	1.346	1.337	1.401	1.394	1.394	1.396	0.985
AEP8	1.346	1.337	1.402	1.393	1.394	1.396	0.984
AEP9	1.347	1.335	1.401	1.395	1.392	1.396	0.985

[a]1 Å = 0.1 nm.

Selected theoretical (DFT) vibrations of AEP conformers. For all stable conformers of AEP, vibrational frequencies were calculated at the DFT(B3LYP)/6-31G* level. The DFT(B3LYP) method, recommended by Scott and Radom [21], has high predictive value, and thus it is frequently used for analysis of experimental IR (and/or Raman) spectra of various molecules [28]. To obtain good agreement with experiment, Palafox [29] proposed a procedure which can be applied to the DFT(B3LYP) computed frequencies. According to this procedure, the following scaling equation was used: $\nu_{scaled} = 0.9519\ \nu_{calculated} + 23.3$.

For our spectral analysis (only the scaled frequencies were taken into account), the stretching NH and CH vibrations, and the bending (in-plane) NH vibrations were selected, *i.e.* all vibrations from the high frequency region (4000–1600 cm^{-1}). The reasons for this selection are as follows. Vibrational frequencies of these groups {particularly the ν(CH) corresponding to the side chain of AEP} are sensitive to conformational changes. In some cases, they vary by 100 cm^{-1} (*vide infra*). Moreover, the ν(NH) and ν(CH) bands can easily be identified in the experimental IR spectrum recorded for AEP in apolar solvent, such as CCl_4 which does not contain the CH group. These bands appear in different frequency regions, which are free from other vibrations, *i.e.* at *ca.* 3500–3300, 3100–3000, and 2980–2780 cm^{-1} for the ν(NH), $\nu(C_{aryl}H)$, and $\nu(C_{alkyl}H)$, respectively [30]. Due to absorption of solvent molecules in the low frequency region (below 1600 cm^{-1}) other stretching and bending vibrations have not been considered in this paper, except the $\delta(NH_2)$ band at 1650–1580 cm^{-1}, which could be analysed only partially.

NH stretching vibrations. For majority of stable conformers of AEP (derivative of primary amine), the stretching NH vibrations (asymmetric and symmetric) do not give significant bands in the DFT calculated IR spectra (Table 3). Only in two *gauche* structures AEP1 (g1) and AEP2 (g2), intramolecular H-bonds between the functional groups, increase the intensity of the $\nu(NH_2)$ bands. This increase of intensity is typical for the associated NH group [30].

Table 3. Stretching NH vibrations[a] for the *gauche* and *trans* conformations of AEP calculated at the DFT(B3LYP)/6-31G* level.

Isomer	Conformation	$\nu^{as}(NH_2)$[b]	$\Delta\nu$[c]	$\nu^{s}(NH_2)$[b]	$\Delta\nu$[c]
AEP1	g1	3545 [3398] (8.4)	16	3456 [3313] (29.3)	6
AEP2	g2	3528 [3382] (6.6)	0	3449 [3307] (7.6)	0
AEP3	g3	3543 [3396] (0.6)	14	3457 [3314] (1.8)	7
AEP4	g4	3546 [3399] (0.7)	17	3463 [3319] (1.7)	12
AEP5	g5	3551 [3403] (0.2)	21	3464 [3321] (1.9)	14
AEP6	t1	3544 [3396] (0.8)	14	3459 [3316] (3.8)	9
AEP7	t2	3542 [3395] (1.0)	13	3456 [3314] (3.1)	7
AEP8	t3	3540 [3393] (0.8)	11	3455 [3312] (1.8)	5
AEP9	t4	3536 [3389] (0.8)	7	3452 [3309] (1.6)	2

[a]Abbreviations for the stretching vibrations: ν^{as} – asymmetric and ν^{s} – symmetric.
[b]Calculated frequency in cm^{-1} [its scaled value] (its intensity in km mol^{-1}).
[c]Relative scaled frequency in cm^{-1}, $\Delta\nu = \nu$(AEPi) – ν(AEP2).

The intramolecular interactions between the chain NH_2 group and the ring N-aza or the ring π electrons influence also the position of both $\nu(NH_2)$ bands. However, this effect is not so strong as in the case of the OH group in alcohols and phenols, for which the associated ν(OH) band can be downshifted even by 200 cm^{-1} [30]. For AEP conformers, the $\nu^{as}(NH_2)$ and $\nu^{s}(NH_2)$ vary from 3403 to 3382 cm^{-1} ($\Delta\nu$ = 21 cm^{-1}) and

from 3321 to 3307 cm^{-1} ($\Delta\nu = 14$ cm^{-1}), respectively, when proceeding from the largest (for g5) to the lowest (for g2) frequency. This downshift (< 50 cm^{-1}) is typical for the intramolecularly H-bonded NH group [30].

NH bending in-plane vibrations. Due to higher intensity (> 10 km mol^{-1}), the bending (scissoring) NH vibrations (in-plane) seems to be more useful than the stretching ones (Table 4). The DFT calculated $\delta(NH_2)$ band is separated from the other bands corresponding to the stretching vibrations of the pyridine ring {the ν(C=C) bands below 1600 cm^{-1}} and to the bending vibrations of the dimethylene group {the $\delta(CH_2)$ bands below 1500 cm^{-1}}. The position of the $\delta(NH_2)$ band varies from 1661 (for the most stable g2 structure) to 1635 cm^{-1} (for g1). In both the *gauche* g1 and g2 structures, the intramolecular H-bonds between the chain NH_2 and the ring N-aza take place.

Table 4. Bending (in-plane) NH vibrations[a] for the *gauche* and *trans* conformations of AEP calculated at the DFT(B3LYP)/6-31G* level.

Isomer	Conformation	$\delta(NH_2)$[b]	$\Delta\delta$[c]
AEP1	g1	1693 [1635] (43.1)	–26
AEP2	g2	1720 [1661] (19.1)	0
AEP3	g3	1702 [1644] (14.2)	–17
AEP4	g4	1698 [1639] (29.2)	–22
AEP5	g5	1697 [1639] (25.6)	–22
AEP6	t1	1698 [1640] (23.3)	–21
AEP7	t2	1696 [1638] (24.7)	–23
AEP8	t3	1701 [1643] (20.6)	–18
AEP9	t4	1702 [1644] (21.6)	–17

[a]Abbreviations for vibrations: δ – bending in-plane (scissoring).
[b]Calculated frequency in cm^{-1} [its scaled value] (its intensity in km mol^{-1}).
[c]Relative scaled frequency in cm^{-1}, $\Delta\delta = \delta$(AEPi) – δ(AEP2).

The different positions of the $\delta(NH_2)$ band in the two intramolecularly H-bonded isomers g1 and g2 suggest that the H-bonds are not the main reason of the $\delta(NH_2)$ band variation ($\Delta\delta = 26$ cm^{-1}). It can be a consequence of different orientation of the NH_2 *vis-á-vis* the CH_2Py group {see Φ_3 angle for g1 (179.0°) and g2 (64.1°) in Table 1, and compare it with that equal to 180° and 60° for the representative conformations of the Φ_3 angle in Fig. 2}. In the g1 structure, the conformation around the terminal C–N bond is similar to that in g4, g5, t1 and t2 (one H of the NH_2 has the *gauche* conformation and the other has the *trans* conformation *vis-á-vis* the CH_2Py group). The position of the $\delta(NH_2)$ band in g1 (1635 cm^{-1}) is also close to that of g4, g5, t1 and t2 (1638–1640 cm^{-1}). The intramolecular H-bonds between the functional groups in g1 only slightly downshift the $\delta(NH_2)$ band (by 3–5 cm^{-1}). In the g2 structure, the conformation around the terminal C–N bond is similar to that in g3, t3 and t4 (both hydrogens of the NH_2 have the *gauche* conformation *vis-á-vis* the CH_2Py group). However, in this conformation, the intramolecular H-bonds between the functional groups in g2

strongly upshift the $\delta(NH_2)$ band (up to 1661 cm^{-1}) in comparison to that found for g3, t3 and t4 (1643–1644 cm^{-1}). This strong upshift (*ca.* 20 cm^{-1}) is very significant and the $\delta(NH_2)$ band may be taken as one of IR markers in detection of the g2 structure.

The intensity of the $\delta(NH_2)$ band in g2 (19.1 km mol^{-1}) is comparable to that in g3, t3 and t4 (14.2, 20.6 and 21.6 km mol^{-1}, respectively) and also to that in g4, g5, t1 and t2 (29.2, 25.6, 23.3 and 24.7 km mol^{-1}, respectively). This means that the intramolecular H-bonds in g2 have no particular influence on the intensity of the $\delta(NH_2)$ band. Quite a different situation occurs in the case of g1. The intensity of the $\delta(NH_2)$ band in g1 is *ca*. twice higher (43.1 km mol^{-1}) than that in the other conformers. These different behaviours in both the intramolecularly H-bonded g1 and g2 structures, *i.e*. high intensity of the $\delta(NH_2)$ band in g1, and strong upshift of the $\delta(NH_2)$ band in g2, indicate how different may the effect of the intramolecular H-bonds be on the $\delta(NH_2)$ band in different conformations of the NH_2 group.

CH stretching vibrations. Rotational isomerism of the aminoethyl group and intramolecular interactions possible in various isomers of AEP significantly influence the stretching CH vibrations of the side chain. In the case of the pyridine ring, these two phenomena have considerably smaller effect. The positions of the four DFT calculated $\nu(C_{aryl}H)$ bands (Table 5) vary from 3088 (for t4) to 3082 (for t1-3), from 3080 (for t4) to 3070 (for g3, t1, t3), from 3059 (for g4, t4) to 3056 (for g3, t1, t3) and from 3040 (for g1) to 3034 cm^{-1} (for g5). The variations ($\Delta\nu$ = 6, 10, 3 and 6 cm^{-1}, respectively) do not exceed 10 cm^{-1}. All these four $\nu(C_{aryl}H)$ bands are very close to each other. Their intensities change from 8.7 (for t4) to 18.5 (for t3), from 22.1 (for g4) to 30.5 (for g5), from 4.9 (for t3) to 11.3 (for g5) and from 24.2 (for g1) to 29.1 km mol^{-1} (for t4), respectively. Although the position and intensity variations are not very significant, all these bands can be taken into account in the interpretation of the experimental IR spectra and in identification of the AEP conformers.

Table 5. Stretching CH vibrations for the pyridine ring in the *gauche* and *trans* conformations of AEP calculated at the DFT(B3LYP)/6-31G* level.

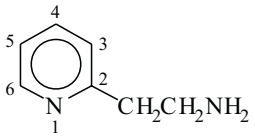

Isomer	Conformation	ν(CH)[a]	$\Delta\nu$[b]	Assignment[c]
AEP1	g1	3215 [3083] (18.1)	–1	$\nu(C^5H)+\nu(C^4H)+\nu(C^3H)$
AEP2	g2	3215 [3084] (16.8)	0	$\nu(C^5H)+\nu(C^4H)$
AEP3	g3	3214 [3083] (17.0)	–1	$\nu(C^5H)+\nu(C^4H)$
AEP4	g4	3214 [3083] (13.8)	–1	$\nu(C^5H)+\nu(C^4H)+\nu(C^3H)$
AEP5	g5	3219 [3088] (9.5)	4	$\nu(C^3H)+\nu(C^4H)+\nu(C^5H)$
AEP6	t1	3213 [3082] (18.4)	–2	$\nu(C^5H)+\nu(C^4H)$

Table 5 (continuation)

AEP7	t2	3213 [3082] (18.2)	–2	$\nu(C^5H)+\nu(C^4H)+\nu(C^3H)$
AEP8	t3	3213 [3082] (18.5)	–2	$\nu(C^5H)+\nu(C^4H)$
AEP9	t4	3220 [3088] (8.7)	4	$\nu(C^3H)+\nu(C^4H)+\nu(C^5H)$
AEP1	g1	3202 [3071] (23.0)	–1	$\nu(C^3H)-\nu(C^5H)+\nu(C^4H)$
AEP2	g2	3203 [3072] (22.8)	0	$\nu(C^3H)-\nu(C^5H)+\nu(C^4H)$
AEP3	g3	3201 [3070] (23.9)	–2	$\nu(C^3H)-\nu(C^5H)+\nu(C^4H)$
AEP4	g4	3206 [3075] (22.1)	3	$\nu(C^3H)-\nu(C^5H)+\nu(C^4H)$
AEP5	g5	3209 [3078] (30.5)	6	$\nu(C^5H)-\nu(C^3H)$
AEP6	t1	3201 [3070] (25.7)	–2	$\nu(C^3H)-\nu(C^5H)+\nu(C^4H)$
AEP7	t2	3202 [3071] (24.1)	–1	$\nu(C^3H)-\nu(C^5H)+\nu(C^4H)$
AEP8	t3	3200 [3070] (24.5)	–2	$\nu(C^3H)-\nu(C^5H)+\nu(C^4H)$
AEP9	t4	3211 [3080] (27.6)	8	$\nu(C^5H)-\nu(C^3H)$
AEP1	g1	3187 [3057] (5.1)	–1	$\nu(C^4H)-\nu(C^3H)$
AEP2	g2	3188 [3058] (5.2)	0	$\nu(C^4H)-\nu(C^3H)$
AEP3	g3	3186 [3056] (5.1)	–2	$\nu(C^4H)-\nu(C^3H)$
AEP4	g4	3189 [3059] (8.1)	1	$\nu(C^4H)-\nu(C^3H)$
AEP5	g5	3188 [3058] (11.3)	0	$\nu(C^4H)-\nu(C^5H)$
AEP6	t1	3186 [3056] (5.4)	–2	$\nu(C^4H)-\nu(C^3H)$
AEP7	t2	3187 [3057] (5.5)	–1	$\nu(C^4H)-\nu(C^3H)$
AEP8	t3	3186 [3056] (4.9)	–2	$\nu(C^4H)-\nu(C^3H)$
AEP9	t4	3190 [3059] (9.8)	1	$\nu(C^4H)-\nu(C^5H)$
AEP1	g1	3169 [3040] (24.2)	1	$\nu(C^6H)$
AEP2	g2	3168 [3039] (24.3)	0	$\nu(C^6H)$
AEP3	g3	3166 [3037] (26.9)	–2	$\nu(C^6H)$
AEP4	g4	3164 [3035] (27.5)	–4	$\nu(C^6H)$
AEP5	g5	3163 [3034] (28.7)	–5	$\nu(C^6H)$
AEP6	t1	3164 [3035] (27.9)	–4	$\nu(C^6H)$
AEP7	t2	3164 [3035] (28.0)	–4	$\nu(C^6H)$
AEP8	t3	3166 [3037] (27.7)	–2	$\nu(C^6H)$
AEP9	t4	3163 [3035] (29.1)	–4	$\nu(C^6H)$

[a]Calculated frequency in cm^{-1} [its scaled value] (its intensity in km mol^{-1}).
[b]Relative scaled frequency in cm^{-1}, $\Delta\nu = \nu(AEPi) - \nu(AEP2)$.
[c]Main vibrations.

In the case of the chain dimethylene group, the variations in the positions and intensities of the four DFT calculated $\nu(C_{alkyl}H)$ bands, corresponding to the asymmetric and symmetric stretching $C^{\alpha}H$ and $C^{\beta}H$ vibrations, are particularly large when proceeding from one to another conformation of AEP (Table 6). Although the $\nu(C_{alkyl}H)$ bands are close to each other, one can indicate the ν(CH) band well separated from the other ones, which can be taken as an IR marker for particular conformation(s).

Table 6. Stretching CH vibrations for the ethylene chain in the *gauche* and *trans* conformations of AEP calculated at the DFT(B3LYP)/6-31G* level.

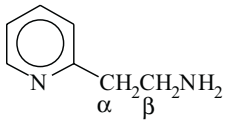

Isomer	Conformation	ν(CH)[a]	$\Delta\nu$[b]	Assignment[c]
AEP1	g1	3081 [2956] (29.9)	–4	$\nu^{as}(C^{\alpha}H_2)$
AEP2	g2	3080 [2955] (41.2)	0	$\nu^{as}(C^{\alpha}H_2)+\nu(C^{\beta}H^{gauche})$
AEP3	g3	3088 [2963] (23.4)	3	$\nu^{as}(C^{\alpha}H_2)+\nu(C^{\beta}H^{gauche})$
AEP4	g4	3112 [2986] (19.2)	26	$\nu^{as}(C^{\alpha}H_2)$
AEP5	g5	3106 [2979] (20.3)	19	$\nu^{as}(C^{\alpha}H_2)$
AEP6	t1	3107 [2981] (28.8)	21	$\nu^{as}(C^{\alpha}H_2)+\nu(C^{\beta}H^{gauche})$
AEP7	t2	3106 [2980] (27.2)	20	$\nu^{as}(C^{\alpha}H_2)$
AEP8	t3	3080 [2955] (8.9)	–5	$\nu^{as}(C^{\alpha}H_2)+\nu(C^{\beta}H^{gauche})$
AEP9	t4	3051 [2928] (4.3)	–32	$\nu^{as}(C^{\alpha}H_2)+\nu(C^{\beta}H^{gauche})$
AEP1	g1	3060 [2936] (57.0)	–19	$\nu(C^{\beta}H^{gauche})$
AEP2	g2	3085 [2960] (45.9)	0	$\nu^{as}(C^{\beta}H_2)+\nu^{as}(C^{\alpha}H_2)$
AEP3	g3	3105 [2979] (33.1)	24	$\nu^{as}(C^{\beta}H_2)$
AEP4	g4	3077 [2952] (63.8)	–3	$\nu(C^{\beta}H^{gauche})$
AEP5	g5	3087 [2962] (26.0)	7	$\nu(C^{\beta}H^{gauche})$
AEP6	t1	3090 [2965] (5.5)	10	$\nu(C^{\beta}H^{gauche})+\nu^{as}(C^{\alpha}H_2)$
AEP7	t2	3066 [2941] (35.4)	–14	$\nu(C^{\beta}H^{gauche})$
AEP8	t3	3109 [2983] (33.5)	28	$\nu^{as}(C^{\beta}H_2)$
AEP9	t4	3086 [2961] (46.3)	6	$\nu^{as}(C^{\beta}H_2)$
AEP1	g1	3035 [2912] (12.4)	–2	$\nu^{s}(C^{\alpha}H_2)$
AEP2	g2	3037 [2914] (20.1)	0	$\nu^{s}(C^{\alpha}H_2)$
AEP3	g3	3040 [2917] (22.7)	3	$\nu^{s}(C^{\alpha}H_2)$
AEP4	g4	3061 [2937] (9.3)	23	$\nu^{s}(C^{\alpha}H_2)$
AEP5	g5	3041 [2918] (27.4)	4	$\nu^{s}(C^{\alpha}H_2)$
AEP6	t1	3043 [2920] (26.1)	6	$\nu^{s}(C^{\alpha}H_2)$
AEP7	t2	3045 [2922] (15.9)	8	$\nu^{s}(C^{\alpha}H_2)$
AEP8	t3	3038 [2915] (20.2)	1	$\nu^{s}(C^{\alpha}H_2)$
AEP9	t4	3026 [2903] (9.1)	–11	$\nu^{s}(C^{\alpha}H_2)$
AEP1	g1	2952 [2833] (85.1)	–85	$\nu(C^{\beta}H^{trans})$
AEP2	g2	3041 [2918] (43.7)	0	$\nu^{s}(C^{\beta}H_2)$
AEP3	g3	3056 [2932] (45.5)	14	$\nu^{s}(C^{\beta}H_2)$
AEP4	g4	2983 [2963] (54.7)	–55	$\nu(C^{\beta}H^{trans})$
AEP5	g5	2962 [2843] (113.9)	–75	$\nu(C^{\beta}H^{trans})$
AEP6	t1	2951 [2832] (82.3)	–86	$\nu(C^{\beta}H^{trans})$
AEP7	t2	2988 [2967] (49.6)	–51	$\nu(C^{\beta}H^{trans})$

Table 6 (continuation)

AEP8	t3	3053 [2929] (40.6)	11	$\nu^{s}(C^{\beta}H_2)$
AEP9	t4	3043 [2920] (42.4)	2	$\nu^{s}(C^{\beta}H_2)$

[a]Calculated frequency in cm^{-1} [its scaled value] (its intensity in km mol^{-1}).
[b]Relative scaled frequency in cm^{-1}, $\Delta\nu = \nu(AEPi) - \nu(AEP2)$.
[c]Symbols for the stretching vibrations: ν^{as} – asymmetric and ν^{s} – symmetric. Symbols for the hydrogens: H^{gauche} – *gauche* position of H *vis-á-vis* the lone electron pair of the chain nitrogen and H^{trans} – *trans* position of H *vis-á-vis* the lone electron pair of the chain nitrogen.

The position and intensity of the $\nu^{as}(C^{\alpha}H_2)$ band or its composite (in phase) with the asymmetric stretching $C^{\beta}H$ or $C^{\beta}H^{gauche}$ vibrations (where H^{gauche} indicates the hydrogen at the C^{β} in the *gauche* position *vis-á-vis* the lone electron pair of the chain N-amino) vary from 2986 (19.2) for g4 through 2955 (45.9) for g2 to 2928 cm^{-1} (4.3) for t4. The variation gives a remarkably wide frequency region ($\Delta\nu$ = 58 cm^{-1}) with the mean ν value of 2965 cm^{-1}. However, this is useless, because the rotation of the chain aminoethyl group influences in the same way the position and intensity of the $\nu^{as}(C^{\beta}H_2)$ and $\nu(C^{\beta}H^{gauche})$ bands or their composites (in phase) with the asymmetric stretching $C^{\alpha}H$ vibrations. They change as follows: from 2983 (33.5) for t3 through 2965 (5.5) for t1 to 2936 cm^{-1} (57.0) for g1. The frequency region is also wide ($\Delta\nu$ = 47 cm^{-1}), and the mean value of 2959 cm^{-1} is close to that found for the $\nu^{as}(C^{\alpha}H_2)$ band (2965 cm^{-1}). The $\nu^{s}(C^{\alpha}H_2)$ band and its intensity are also useless. They vary as follows: from 2937 (9.3) for g4 through 2918 (27.4) for g5 to 2903 cm^{-1} (9.1) for t4. The frequency region ($\Delta\nu$ = 34 cm^{-1}) is not so wide as for the asymmetric stretching $C^{\alpha}H$ vibrations, but the mean ν value of 2918 cm^{-1} is separated from that (2959 cm^{-1}) for the asymmetric stretching $C^{\beta}H$ vibrations by 41 cm^{-1}. This means that the largest value of the $\nu^{s}(C^{\alpha}H_2)$ band (2937 cm^{-1} for g4) is close to the lowest value of the $\nu^{as}(C^{\alpha}H_2)$ (2928 cm^{-1} for t4) and $\nu(C^{\beta}H^{gauche})$ bands (2936 cm^{-1} for g1). The same is true for the $\nu^{s}(C^{\beta}H_2)$ band found for g2, g3, t3 and t4. It varies from 2932 (for g3) to 2918 cm^{-1} (for g2). Although the frequency region ($\Delta\nu$ = 14 cm^{-1}) is narrow, the mean ν value of 2925 cm^{-1} is close to that for the $\nu^{s}(C^{\alpha}H_2)$ band (2918 cm^{-1}). The intensity of the $\nu^{s}(C^{\beta}H_2)$ band does not depend on conformation and it is close to *ca.* 43 km mol^{-1}.

One exception is the $\nu(C^{\beta}H^{trans})$ band, where H^{trans} indicates the hydrogen at the C^{β} in the *trans* position *vis-á-vis* the lone electron pair of the chain N-amino. The position and intensity of the $\nu(C^{\beta}H^{trans})$ band change from 2867 (49.6) and 2863 (54.7) for t2 and g4 through 2843 (113.9) for g5 to 2833 (85.1) and 2832 cm^{-1} (82.3) for g1 and t1. This band is separated from the other ones by *ca.* 40–70 cm^{-1} and its intensity is very significant. Thus the $\nu(C^{\beta}H^{trans})$ band can be used as an IR marker for identification of the g1, g4, g5, t1 and t2 structures in the mixture of the AEP isomers.

Experimental FT-IR spectrum of AEP in apolar solvent. Four frequency regions of the FT-IR spectrum, corresponding to the stretching NH, $C_{aryl}H$ and $C_{alkyl}H$ vibrations and to the bending (in-plane) NH vibrations were selected to study the conformational preferences of AEP in CCl_4. They are shown in Fig. 4. Preliminary analysis of these regions indicates that AEP does not exists in one conformation in apolar solvent. The $\nu(NH)$, $\delta(NH_2)$, $\nu(C_{aryl}H)$, and $\nu(C_{alkyl}H)$ contours consist of few compo-

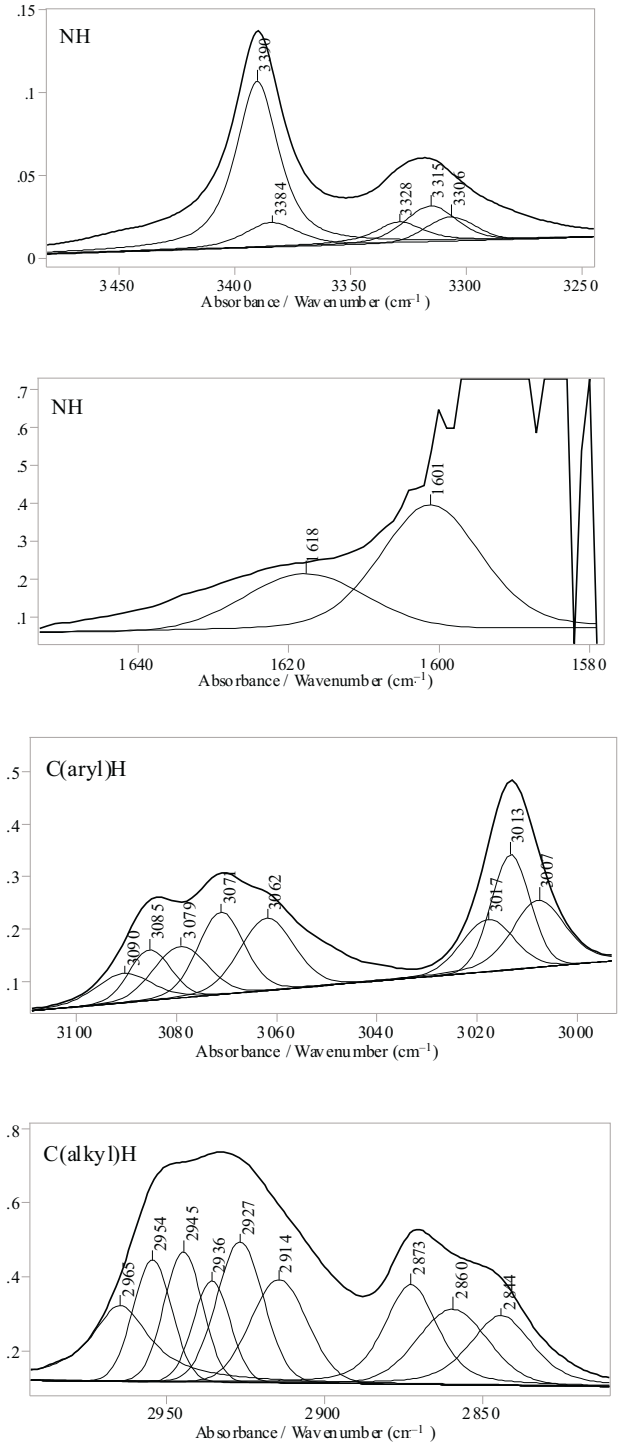

Figure 4. Frequency regions selected from the experimental FT-IR spectra of AEP in CCl_4 solution (0.02 mol dm^{-3} in 2.66 mm KBr cell).

nent bands. Change of concentration of AEP in CCl_4 solutions from 0.001 to 0.1 mol dm^{-3} has only slight influence on the positions of all selected bands.

Taking into account this observation and the DFT calculated IR spectra for the nine isomers of AEP, the experimental $\nu^{as}(NH_2)$ and $\nu^{s}(NH_2)$ contours were decomposed into two (at 3390 and 3384 cm^{-1}) and three (at 3328, 3315 and 3306 cm^{-1}) component bands, respectively. The component $\nu^{as}(NH_2)$ band at larger frequency refers to all AEP isomers except g2, and that at lower frequency to g2 (Table 3). The component $\nu^{s}(NH_2)$ band at larger frequency corresponds to g4 and g5, that at middle frequency to g1, g3, and t1-t3, and that at lower frequency to g2 and t4. The intensities of these component bands are significant and suggest that all isomers of AEP can be present in CCl_4 solution.

According to the DFT calculations, the $\delta(NH_2)$ contour could be decomposed into four component bands corresponding to g2 (at *ca.* 1660 cm^{-1}), g3, t3 and t4 (at *ca.* 1644 cm^{-1}), g4, g5, t1 and t2 (at *ca.* 1639 cm^{-1}), and g1 (at *ca.* 1635 cm^{-1}), respectively (Table 4). Unfortunately, the experimental $\delta(NH_2)$ contour is downshifted (by *ca.* 40 cm^{-1}) in comparison to the DFT calculated bands towards the ν(C=C) frequency region for the pyridine ring and to the solvent absorption region. Therefore, the decomposition of the $\nu(NH_2)$ contour is difficult. One can only indicate the partial band at larger frequency (at *ca.* 1620 cm^{-1}), which can be assigned to the (NH_2) band of g2.

The ν(CH) bands are well separated from the other bands, and they have significant intensities. In the case of very broad experimental $\nu(C_{aryl}H)$ contour at larger frequency, five component bands were distinguished (at 3090, 3085, 3079, 3071 and 3062 cm^{-1}). According to the DFT calculations (Table 5), the two component $\nu(C_{aryl}H)$ bands at larger frequencies correspond to the stretching CH vibrations in phase: $\nu(C^3H)+\nu(C^4H)+\nu(C^5H)$ for g5 and t4, and $\nu(C^5H+\nu(C^4H)+\nu(C^3H)$ for g1-g4 and t1-t3. The other three $\nu(C_{aryl}H)$ component bands refer to the stretching CH vibrations in counter-phase: $\nu(C^5H)–\nu(C^3H)$ for g5 and t4, $\nu(C^3H)–\nu(C^5H)+\nu(C^4H)$ for g1-g4 and t1-t3, and $\nu(C^4H)–\nu(C^3H)$ or $\nu(C^4H)–\nu(C^5H)$ for all nine isomers. Their intensities are significant, similarly as those computed at the DFT level. The same is true for the other experimental $\nu(C_{aryl}H)$ contour at lower frequency corresponding to the stretching C^6H vibrations, for which three component bands were distinguished (at 3017, 3013 and 3007 cm^{-1}). The component $\nu(C^6H)$ band at larger frequency refers to g1 and g2, that at middle frequency to g3 and t3, and that at lower frequency to g4, g5, t1, t2 and t4. Their intensities are also significant and suggest that all nine isomers of AEP exist in CCl_4 solution.

In the case of very broad experimental $\nu(C_{alkyl}H)$ contour at larger frequency, six component bands were distinguished (at 2965, 2954, 2945, 2936, 2927 and 2914 cm^{-1}). According to the DFT calculations, they correspond to the asymmetrical and symmetrical stretching $C^{\alpha}H$ and $C^{\beta}H$ vibrations for various AEP isomers (Table 6). Their intensities are significant, similarly as those computed at the DFT level for AEP isomers.

Important conclusion can be derived on the basis of the other experimental contour of high intensity at lower frequency of the $\nu(C_{alkyl}H)$ region. An appearance of bands below 2900 cm^{-1} are usually attributed to overtone vibrations, and/or to various combination tones, corresponding to the sum or difference of the fundamental frequencies. However, these overtones and combinations have low intensity [30]. Therefore, one can conclude that the experimental, intense $\nu(C_{alkyl}H)$ contour at lower frequency corresponds mainly to the stretching $C^{\beta}H^{trans}$ vibrations. Taking into account this conclusion and the DFT calculations, this contour can be decomposed at least into three component bands. The component $\nu(C^{\beta}H^{trans})$ band at larger frequency (2873 cm^{-1}) refers to g4 and t2, that at middle frequency (2860 cm^{-1}) to g5, and that at lower frequency (2844 cm^{-1}) to g1 and t1 (Table 6). High intensities of these partial bands suggest that the g1, g4, g5, t1 and t2 structures exist in CCl_4 solution.

CONCLUSIONS

Among one hundred conformers considered for AEP, nine stable structures have been found at the DFT(B3LYP)/6-31G* level. Most of them are similar to those found for the T_1 tautomer of histamine. This conformational similarity between AEP and HA can partially explain similarity of both ligands in binding with the H_1 receptor. Differences between the Gibbs energies of nine AEP isomers are not larger than 1.5 kcal mol^{-1}, and difference in their polarities are smaller than 2 Debyes. Aromatic character of the pyridine moiety measured by the HOMA index does not depend on conformation of the aminoethyl group and it is close to unity for all nine isomers of AEP. Smaller aromatic character of the imidazole ring in histamine (HOMA = 0.85 ± 0.05) and higher polarity of HA than AEP can explain differences in physiological and behavioural effects of both ligands and their different affinities in binding with the H_1 receptor.

Rotational isomerism of the side chain and intramolecular interactions between the chain amino group and the aza or π electrons in the pyridine ring significantly influence the calculated vibrational frequencies, especially the stretching CH vibrations of the aminoethyl group. The DFT calculated $\nu(C^{\beta}H^{trans})$ for AEP1 and AEP4-AEP7 is separated from the other ν(CH) bands by 40–70 cm^{-1}. On the other hand, the $\delta(NH_2)$ band for AEP2 is upshifted by *ca.* 20 cm^{-1} in comparison to that for other isomers. These observations have been very useful in interpretation of the experimental IR spectrum of AEP recorded in CCl_4 solution. Significant intensities of all component ν(NH) and ν(CH) bands suggest that AEP exists as a mixture of its rotational isomers in apolar solvent.

Acknowledgments

Ab initio calculations were carried out at the Interdisciplinary Center for Molecular Modeling (ICM, Warsaw).

REFERENCES

1. Fossati A., Barone D. and Benvenuti C., *Pharmacol. Res*., **43**, 389 (2001).
2. a) Tran V.T., Chang R.S.L. and Snyder S.H., *Proc. Natl. Acad. Sci. USA*, **75**, 6290 (1978); b) Eckman D.M., Hopkins N., McBride C. and Keef K.D., *Br. J. Pharmacol*., **124**, 181 (1998).
3. a) Ganellin C.R., In *Pharmacology of Histamine Receptors*, Ganellin C.R., Parsons M.E. (Eds.), Wright PSG, Bristol, 1982, p. 9; b) Cooper D.G., Vong R.C., Durant G.J. and Ganellin C.R., In *Comprehensive Medicinal Chemistry*, Jammes P.G., Taylor J.B. (Eds.), Pergamon Press, Oxford, 1990, vol. 3, p. 323.
4. Leurs R., Hoffman M., Wieland K. and Timmerman H., *Trends Pharmacol. Sci*., **21**, 11 (2000).
5. Weinstein H., Chou D., Johnson C.L., Kang S. and Green J.P., *Mol. Pharmacol*., **12**, 738 (1976).
6. Weinstein H., Mazurek A.P., Osman R. and Topiol S., *Mol. Pharmacol.*, **29**, 28 (1986).
7. Karpińska G. and Mazurek A.P., *Z. Naturforsch*., **50c**, 143 (1995).
8. Raczyńska E.D., Cyrański M.K., Darowska M. and Rudka T., *Targets in Heterocycl. Syst. Chem. Prop.*, **4**, 327 (2000), and references cited therein.
9. Raczyńska E.D., Maria P.-C., Gal J.-F. and Decouzon M., *J. Phys. Org. Chem*., **7**, 725 (1994).
10. Raczyńska E.D., Rudka T. and Darowska M., *J. Mol. Struct. (Theochem)*, **574**, 221 (2001).
11. Raczyńska E.D., Darowska M., Rudka T., and Makowski M., *J. Phys. Org. Chem*., **14**, 770 (2001).
12. Darowska M. and Raczyńska E.D., *Polish J. Chem*., **76**, 1027 (2002).
13. Hernández-Laguna A., Abboud J.-L.M., Notario R., Homan H. and Smeyers Y.G., *J. Am. Chem. Soc*., **115**, 1450 (1993).
14. Collado J.A., Tuñón I., Silla E. and Ramírez F.J., *J. Phys. Chem. A*, **104**, 2120 (2000).
15. Paesen G.C., Adams P.L., Nuttall P.A. and Stuart D.L., *Biochim. Biophys. Acta*, **1482**, 92 (2000).
16. a) NCBI (National Center for Biotechnology Information), http://www.ncbi.nlm.nih.gov; b) Protein Data Bank, http://pdb.ccdc.cam.ac.uk/pdb/.
17. Dewar M.J.S., Zoebisch E.G., Healy E.F. and Stewart J.J.P., *J. Am. Chem. Soc*., **107**, 3902 (1985).
18. Parr R.G and Yang W., *Density Functional Theory of Atoms and Molecules*, Oxford University Press, NY, 1989.
19. a) Becke A.D., *J. Chem. Phys*., **98**, 5648 (1993); b) Lee C., Yang W. and Parr R.G., *Phys. Rev. B*, **37**, 785 (1988).
20. Hehre W.J., Radom L., Schleyer P.v.R. and Pople J.A., *Ab Initio Molecular Theory*, Wiley, NY, 1986.
21. Scott A.P and Radom L., *J. Phys. Chem*., **100**, 16502 (1996).
22. Frisch M.J., Trucks G.W., Schlegel H.B., Gill P.M.W., Johnson B.G., Robb M.A., Cheeseman J.R., Keith T.A., Petterson G.A., Montgomery J.A., Raghavachari K., Al-Laham M.A., Zakrzewski V.G., Ortiz J.V., Foresman J.B., Ciosłowski J., Stefanov B., Nanayakkara A., Challacombe M., Peng C.Y., Ayala P.Y., Chen W., Wong M.W., Andres J.L., Replogle E.S., Gomperts R., Martin R.L., Fox D.J., Binkley J.S., DeFrees D.J., Baker J., Stewart J.P., Head-Gordon M., Pople J.A., Gaussian, Inc., Pittsburgh, PA, 1995.
23. Schaftenaar G. and Noordik J.H., *J. Comput.-aided Mol. Des*., **14**, 123 (2000).
24. Godfrey P.D. and Brown R.D., *J. Am. Chem. Soc*., **120**, 10724 (1998), and references cited therein.
25. Krygowski T.M., *J. Chem. Inf. Comput. Sci*., **33**, (1993).
26. Krygowski T.M., Cyrański M.K., Czarnocki Z., Häfelinger G. and Katritzky A.R., *Tetrahedron*, **56**, 1783 (2000).
27. Krygowski M.K. and Cyrański M.K., *Chem. Rev.*, **101**, 1385 (2001).
28. a) Jamróz M.H., Dobrowolski J.Cz., Rode J.E. and Borowiak M.A.,*J. Mol. Struct. (Theochem)*, **618**, 101 (2002); b) Rode J.E., Dobrowolski J.Cz., Borowiak M.A. and Mazurek A.P., *Phys. Chem. Chem. Phys*., **4**, 3948 (2002).
29. Palafox A.M., *Int. Quantum Chem*., **77**, 661 (2000).
30. Wojtkowiak B. and Chabanel M., *Spectrochimie Moleculaire*, Technique et Documentation, Paris, 1977.